RESEARCH ARTICLE

Influence of the stoichiometric ratio on the in-situ formation of crystals and the mechanical properties of epoxy resin cured with L-tyrosine

Florian Rothenhäusler [ID] | Holger Ruckdaeschel [ID]

Department of Polymer Engineering, University of Bayreuth, Bayreuth, Germany

Correspondence
Holger Ruckdaeschel, Department of Polymer Engineering, University of Bayreuth, Universitätsstr. 30, 95447 Bayreuth, Germany.
Email: holger.ruckdaeschel @uni-bayreuth.de

Abstract

One of the most influential ways to alter the network structure of thermosets is to change the stoichiometric ratio (R) between the functional groups of the resin and curing agent. Therefore, the influence of the stoichiometric ratio on the network structure and mechanical properties of diglycidyl ether of bisphenol A (DGEBA) cured with L-tyrosine was investigated with the goal to derive structure–property relationships. Mixtures of DGEBA and L-tyrosine were prepared using three-roll milling, with stoichiometric ratios ranging from $0.9 < R < 1.5$. Upon increasing R, a greater abundance of L-tyrosine crystals was observed, serving as reinforcements within the epoxy matrix. As a result, the network structure and glass transition temperature displayed only marginal changes compared to epoxy resins cured with conventional amine curing agents. Notably, the flexural strength and strain at failure exhibited insignificant variations. Interestingly, the addition of additional L-tyrosine to the resin resulted in an augmented fracture toughness, indicating the toughening capabilities of L-tyrosine crystals. As a result, the amino acid acts not only as a curing agent but also as a toughening agent. Consequently, further incorporation of L-tyrosine into the thermoset proved advantageous, enhancing its overall mechanical performance.

Highlights

- Proofing the existence of amino acid crystals in the epoxy matrix
- Showing that over-stoichiometric ratios result in more amino acid crystals
- Demonstrating that the network structure and T_g change only slightly
- L-tyrosine crystals act as toughening agents and increase fracture toughness
- Structure–property relationships between R and mechanical properties

KEYWORDS

bio-based, epoxy resin, mechanical properties, network structure, stoichiometric ratio, toughening

1 | INTRODUCTION

Epoxy resin-based thermosets play a crucial role as matrix materials in fiber-reinforced polymer composites due to their favorable mechanical properties, high glass transition temperatures (T_g), and low viscosity during fiber impregnation.[1,2] The properties of these thermosets are primarily dictated by the molecular structures of the resin and curing agent, including the type, number, and spatial arrangement of functional groups.[3,4] Moreover, the network structure is influenced by the stoichiometric ratio (R) of functional groups present in the resin and curing agent, such as the ratio of the number of active hydrogen atoms in an amine curing agent to the number of epoxy groups in the resin. This stoichiometric ratio has a direct impact on the cross-link density (ν_C), which, in turn, is a significant characteristic of the overall network structure of the thermosets.[5–7] The cross-link density refers to the density of chemical cross-links in a thermoset formed between the resin and curing agent and is influenced by factors such as the molecular weight of the resin and curing agent, as well as their functionality. Given the significant influence of R on the network structure, its precise tuning becomes essential for tailoring the desired mechanical properties of the thermosets.

Therefore, Murayama et al. investigated the influence of the stoichiometric ratio on the cross-link density and the T_g in diamine-cured epoxy resin. Here, $R > 1$ leads to a decreased ν_C and T_g as well as a decreased storage modulus below and above T_g.[8] A similar investigation by Gupta et al. showed that ν_C and T_g are maximum at $R = 1$ whereas the modulus is minimal at $R = 1$.[9] The modulus increases for $R \neq 1$ due to the steric hindrance of unreacted groups in the epoxy resin and curing agent. Furthermore, the tensile strength slightly increases for $R > 1$ compared to $R = 1$. Interestingly, the critical stress intensity factor in mode I (K_{IC}) is maximal at R slightly greater than one and decreases significantly if $R \ll 1$. The influence of R on the T_g and modulus was confirmed by Palmese et al. who investigated diglycidyl ether of bisphenol A cured with 4,4′-methylenebis(cyclohexylamine).[10] Meyer et al. investigated, among other things, the influence of R on the flexural properties of DGEBA cured with 4,4′-diaminodiphenylsulfone. Here, the flexural modulus and strength are minimal at $R = 1$ whereas the flexural strain at failure increases for $R > 1$.[11] Similarly, Fernandez-Nograro et al. found that the flexural modulus and strength are maximal for $R = 0.8$ to 0.9, while strain to failure increases with increasing R. The fracture energy (G_{IC}) was maximal at $R \sim 1$.[12]

In light of the growing demand for sustainable alternatives in epoxy-based thermosets, the exploration of amino acids as potential substitutes for amine curing
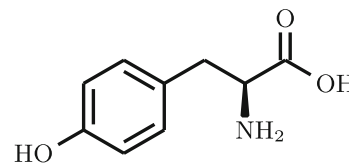

FIGURE 1 Chemical structure of L-tyrosine.

agents has gained attention. Amino acids offer several advantages as they are derived from renewable resources, biodegradable, and non-toxic.[13,14] Surprisingly, previous studies have paid limited attention to the influence of R on the resulting mechanical properties. In some cases, researchers either did not specify the stoichiometric ratio employed in their investigations,[15] or focused solely on a fixed ratio, such as $R = 1$.[16–20]

In contrast to these approaches, Mazzochetti et al. and Merighi et al. utilized a weight ratio of 75% DGEBA and 25% L-tryptophan, resulting in $R = 0.837$ for their investigations.[21,22] Li et al. explored different molar ratios of DGEBA to L-tryptophan and found that a ratio of 3:1 yielded the highest T_g of 107°C.[23] Interestingly, Motahari et al. investigated the same molar ratios and reported that a molar ratio of 2:1 resulted in the highest T_g of 102°C.[24] Most notably, the effect of undissolved amino acid particles in the epoxy resin on the mechanical properties of thermosets remains to be investigated. In conclusion, the effect of the ratio between functional groups of the epoxy resin and the amino acid curing agent on the mechanical properties of thermosets has not been addressed sufficiently in literature.

The primary objective of this study is to analyze the impact of the stoichiometric ratio on various properties, including the degree of crystallinity, T_g, ν_C, flexural properties, and fracture toughness of DGEBA cured with L-tyrosine (see Figure 1). By establishing structure–property relationships, this investigation aims to enhance our understanding of the properties exhibited by epoxy resins cured with amino acids. The ultimate goal is to identify the stoichiometric ratio that strikes a favorable balance between achieving high T_g, optimal flexural strength, and desirable fracture toughness properties.

2 | EXPERIMENTAL

2.1 | Materials

D.E.R. 331 with an epoxide equivalent weight of 187 g/mol was purchased from Blue Cube Assets GmbH & Co. KG, Olin Epoxy (Stade, Germany). L-tyrosine was purchased from Buxtrade GmbH (Buxtehude, Germany) and is provided as coarse powder. L-tyrosine was chosen as the curing agent because a previous study about the mechanical

properties of amino acid cured epoxy resins showed that it resulted in the thermoset with the highest T_g and Young's modulus.[19] 2-Ethyl-4-methyl-imidazole (2E4M-imidazole) with a purity of 95% was bought from Tokyo Chemical Industry Co., Ltd. (Tokyo, Japan).

2.2 | Resin formulation

For this study, six different mixtures were prepared with stoichiometric ratios ranging from 0.9 to 1.5. The preparation process followed the three-roll milling procedure described in detail in a previous work by Rothenhäusler et al.[17] In this study, it was assumed that L-tyrosine possesses three active hydrogen atoms, resulting in an active hydrogen equivalent weight of 60.4 g/mol. It was assumed that the hydroxyl group of L-tyrosine is hindered by the face-to-face dimer which L-tyrosine usually forms in its crystalline form. Therefore, only three active hydrogen atoms are present. To initiate the curing process, 1 weight percentage of the accelerator, specifically 2-ethyl-4-methyl-imidazole, was added to the mixture (Table 1). The mixing step was performed using a centrifuge speed mixer from Hauschild Engineering (Hamm, Germany) at a speed of 3000 1/min for a duration of 120 s. Subsequently, the mixture was subjected to a degassing process for 30 min at a pressure of 10 mbar to ensure the removal of any entrapped air before curing.

It is important to note that the data for the mixture with a stoichiometric ratio of $R = 1$, referred to as T10, was obtained from a previous investigation conducted by Rothenhäusler et al.[19]

2.3 | Curing cycle and sample preparation

To proceed with the experiment, the amino acid epoxy mixture was carefully poured into pre-heated aluminum molds, which had been heated to 60°C. Curing of the thermoset took place in a Memmert ULE 400 convection oven

from Memmert GmbH + Co. KG (Schwabach, Germany) for a total duration of 2 h at 120°C, followed by an additional 2 h at 170°C. After the curing process, the molds were allowed to cool gradually over a period of 4 h to reach room temperature, thus minimizing the development of internal stresses within the specimens. To prepare the specimens for testing, a Mutronic DIADISC5200 diamond plate saw from MUTRONIC Präzisionsgerätebau GmbH & Co. KG (Rieden am Forggensee, Germany) was utilized, adhering to the relevant test method standards.

2.4 | Measurements and characterization

2.4.1 | Differential scanning calorimetry

Dynamic differential scanning calorimetry (DSC) measurements were used to determine the temperature at which the endothermic peak is maximal as well as the melting enthalpy H_m of the different compositions. Here, a Mettler Toledo DSC 1 (Columbus, Ohio, USA) was employed with a heating rate of 10 K/min from 25°C to 330°C. The flow of nitrogen was set to 50 mL/min. The sample mass was $15 +- 2$ mg. Two specimens were tested to ensure sufficient reproducibility. The degree of crystallinity (X_c) was calculated as:

$$X_c = \frac{H_m}{H_0},\tag{1}$$

with the melting enthalpy of the respective composition H_m and the melting enthalpy of the pure crystalline phase H_0 which is 765.5 J/g according to Ji et al.[25]

2.4.2 | Scanning Electron Microscopy

For the characterization of the fracture surfaces of the compact tension specimens, a Zeiss Gemini 1530 Scanning Electron Microscope (SEM) from Carl Zeiss AG

TABLE 1 Compositions of mixtures of DGEBA and L-tyrosine with different R values.

Label	R	DGEBA [wt.%]	L-tyrosine [wt.%]	2E4M-imidazole [wt.%]
T09	0.9	76.7	22.3	1
T10	1.0	74.8	24.2	1
T11	1.1	73.0	26.0	1
T12	1.2	71.3	27.7	1
T13	1.3	69.7	29.3	1
T14	1.4	68.2	30.8	1
T15	1.5	66.7	32.3	1

FIGURE 2 DSC thermograms of DGEBA cured with different R of L-tyrosine after curing.

FIGURE 3 Concentration of L-tyrosine in the formulation C_{tyrosine} and the resulting degree of crystallinity X_c of DGEBA cured with different R of L-tyrosine.
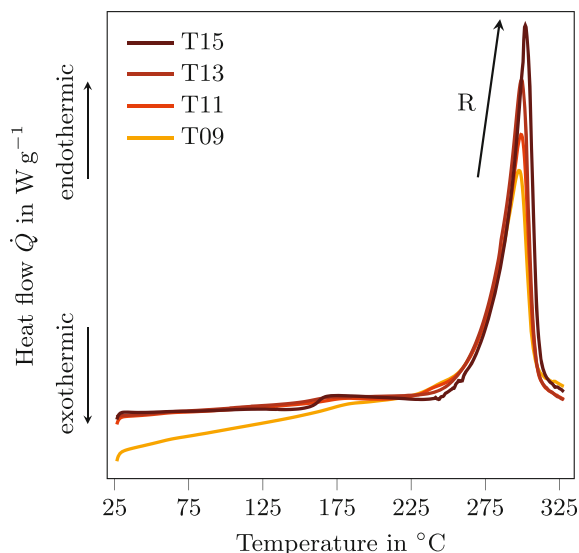
(Oberkochen, Germany) was employed. The SEM analysis was conducted using an acceleration voltage of 3 kV. To enhance the conductivity and minimize charging effects, the surfaces of the specimens were coated with a thin layer of platinum through a sputtering process. The platinum coating had an approximate thickness of 5 nm.

2.4.3 | Dynamic mechanical analysis (DMA)

For investigating the thermosets' thermo-elastic properties, dynamic mechanical analysis was carried out on a Gabo Eplexor 500 N (Gabo Qualimeter Testanlagen GmbH Ahlden, Germany) in tension mode. The specimens with dimensions 50 mm by 10 mm by 2 mm were measured from −120°C to 240°C with a constant heating rate of 3 K/min. The tensile force amplitude was set to 60 N with a frequency of 1 Hz. Here, T_g was taken as the temperature of the maximum value of the loss factor $\tan\delta$. The thermosets' ν_C was calculated as:

$$\nu_c = \frac{E'}{3RT},\tag{2}$$

with the storage modulus (E') at $T = T_g + 50$ K and the universal gas constant $R = 8.314$ J/mol × K.[6] Three specimens were tested to ensure reproducibility of the results.

2.4.4 | Three-point bending

For the three-point bending tests, eight specimens with dimensions 80 mm by 10 mm by 4 mm of each
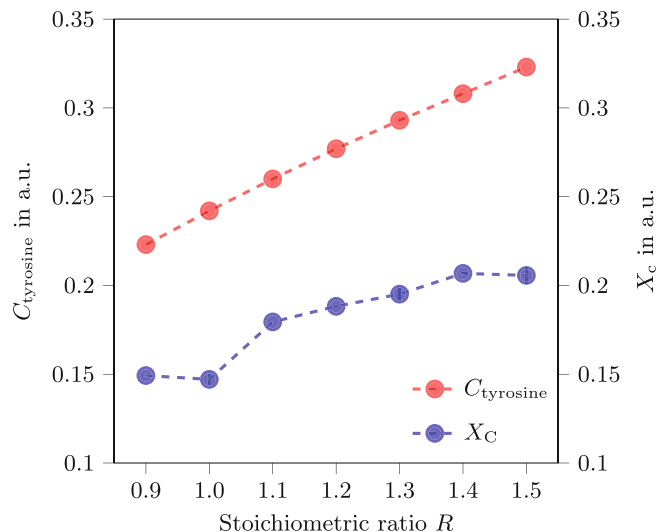
composition were tested with a cross-head speed of 2 mm/min according to ISO 178. The three-point bending tests were carried out on a ZwickRoell Z2.5 universal testing machine by ZwickRoell GmbH & Co. KG (Ulm, Germany) using a load cell with a capacity of 2.5 kN.

2.4.5 | Fracture toughness

K_{IC} and G_{IC} were determined by testing eight compact tension specimens according to ISO 13586 on a ZWICK Z2.5 by ZwickRoell GmbH & Co. KG (Ulm, Germany). The G_{IC} values are calculated from the K_{IC} values via:

$$G_{IC} = \frac{K_{IC}^2}{E_F} \cdot \left(1 - \nu^2\right)\tag{3}$$

with flexural modulus (E_F) taken from the three-point bending tests and Poisson's ratio (ν), which is about 0.35 in the thermoset's glassy state.[26]

3 | RESULTS AND DISCUSSION

3.1 | Differential scanning calorimetry

In order to investigate the influence of R, or the increased weight fraction of the amino acid curing agent, on the mechanical properties of epoxy resin cured with L-tyrosine, it is crucial to analyze and discuss the crystal formation. To validate the presence of crystals observed in

Section 3.2, dynamic DSC measurements are conducted on the cured thermosets (see Figure 2). The DSC thermograms exhibit an endothermic peak during the initial heating cycle at approximately 300°C, consistent with the findings of Ji et al. for pure L-tyrosine crystals (312°C).[25] This endothermic heat flow corresponds to the energy required to "melt" or degrade the amino acid crystals, resulting in the release of volatile compounds with low molecular weight, such as water, ammonia, and CO_2.[27]

Based on the images presented in Section 3.2, it is evident that the amino acid crystals are embedded within the epoxy matrix. This discovery marks the first report of amino acid crystal formation in epoxy resins cured with amino acids in the literature. This phenomenon may explain the differing results obtained by Li et al. and Motahari et al. when investigating the effect of the molar ratio between DGEBA and L-tryptophan on the T_g. Li et al. ground L-tryptophan into a fine powder prior to their DSC measurements, without specifying the method used or the resulting particle size distribution.[23] In contrast, Motahari et al. dissolved the resin systems in acetone, likely resulting in the molecular distribution of L-tryptophan within the matrix, rather than in particle form.[24] The molecular distribution likely suppressed crystal formation and facilitated the curing reaction between L-tryptophan and DGEBA. Consequently, Li et al. needed to add a higher amount of amino acid to their mixtures because either the particle size they used was not small enough for the particles to significantly participate in the curing process, or the larger particles formed crystals.

Figure 3 illustrates the concentration of L-tyrosine in the formulation ($C_{tyrosine}$) and the resulting X_c of DGEBA cured with different R values of L-tyrosine. Naturally, $C_{tyrosine}$ increases linearly with R (see Table 1). In general, X_c increases as R increases, ranging from 14.9% (T09) to 20.6% (T15). Consequently, a significant portion of the thermoset comprises crystalline L-tyrosine. Further evidence for the existence of amino acid crystals within the thermoset matrix is discussed in Section 3.2.

The difference between $C_{tyrosine}$ and X_c can be interpreted as the amount of L-tyrosine that is actually utilized as a curing agent for the epoxy resin ($C_{tyrosine,cure}$). Notably, this difference is relatively consistent across all tested formulations. However, $C_{tyrosine,cure}$ increases as R increases since crystal formation is a kinetic process that requires time. With higher L-tyrosine content in the epoxy matrix, more time is needed for the diffusion of the amino acid within the matrix, subsequent separation of the amino acid from the epoxy resin, and growth of amino acid crystals.[28,29] These processes are hindered by the increasing viscosity of the resin systems as R increases due to its particulate suspension nature.[30,31]

The average difference across all formulations is approximately 9.34% ± 1.32, which corresponds to an R value of 0.32. Consequently, significantly less L-tyrosine is incorporated into the thermoset network during curing than expected. The pronounced crystal formation could be attributed to the low solubility of L-tyrosine in DGEBA or the imidazole accelerator that promotes the homopolymerization of epoxy groups.[32] Therefore, epoxy resins utilizing L-tyrosine, and potentially other amino acids as well, as curing agents cannot be cured in a stoichiometric ratio of $R = 1$. It can be assumed that the excess epoxy groups react with either the accelerator or with hydroxyl groups formed during the reaction between amino and epoxy groups.

3.2 | Scanning Electron Microscopy

The analysis of crystal size and morphology of L-tyrosine crystals is crucial for understanding their impact on the mechanical properties of the epoxy resin. Figure 4 presents SEM images of the fracture surface of a compact tension specimen made from T10 ($R = 1$) at different magnifications.

Figure 4A provides an overview of the rough and complex surface structure of T10. It reveals particles of various length scales, ranging from a few micrometers to over 30 μm in length, with the largest particles having a thickness of about 10 μm. It is important to note that these visible particles represent only a portion of the amino acid crystals on the fracture surface, and the crystals could be even larger. This observation is remarkable considering that the gap widths used during the preparation of the DGEBA and L-tyrosine mixture using a three-roll mill were 25 and 5 μm, respectively. Therefore, the gap widths were significantly smaller than the L-tyrosine crystals. Typically, the smallest observable amino acid particles in cured thermosets range from 50 nm to 100 nm in size.[17] This indicates that the crystals in Figure 4 formed from individual amino acid molecules or smaller particles of L-tyrosine.

While Rothenhäusler et al. also observed coarse fracture surfaces in their investigation of DGEBA cured with L-arginine, they did not mention agglomeration or particle formation.[18] However, at the time of their study, they were not aware of the possibility of crystal formation. Ji et al. demonstrated that L-tyrosine can form crystals with face-to-face dimers of L-tyrosine as building blocks.[25] They presented L-tyrosine crystals with a thickness ranging from 1 μm to 10 μm, which is consistent with the particles observed in Figure 4. The crystalline nature of the particles is further confirmed in Section 3.1.
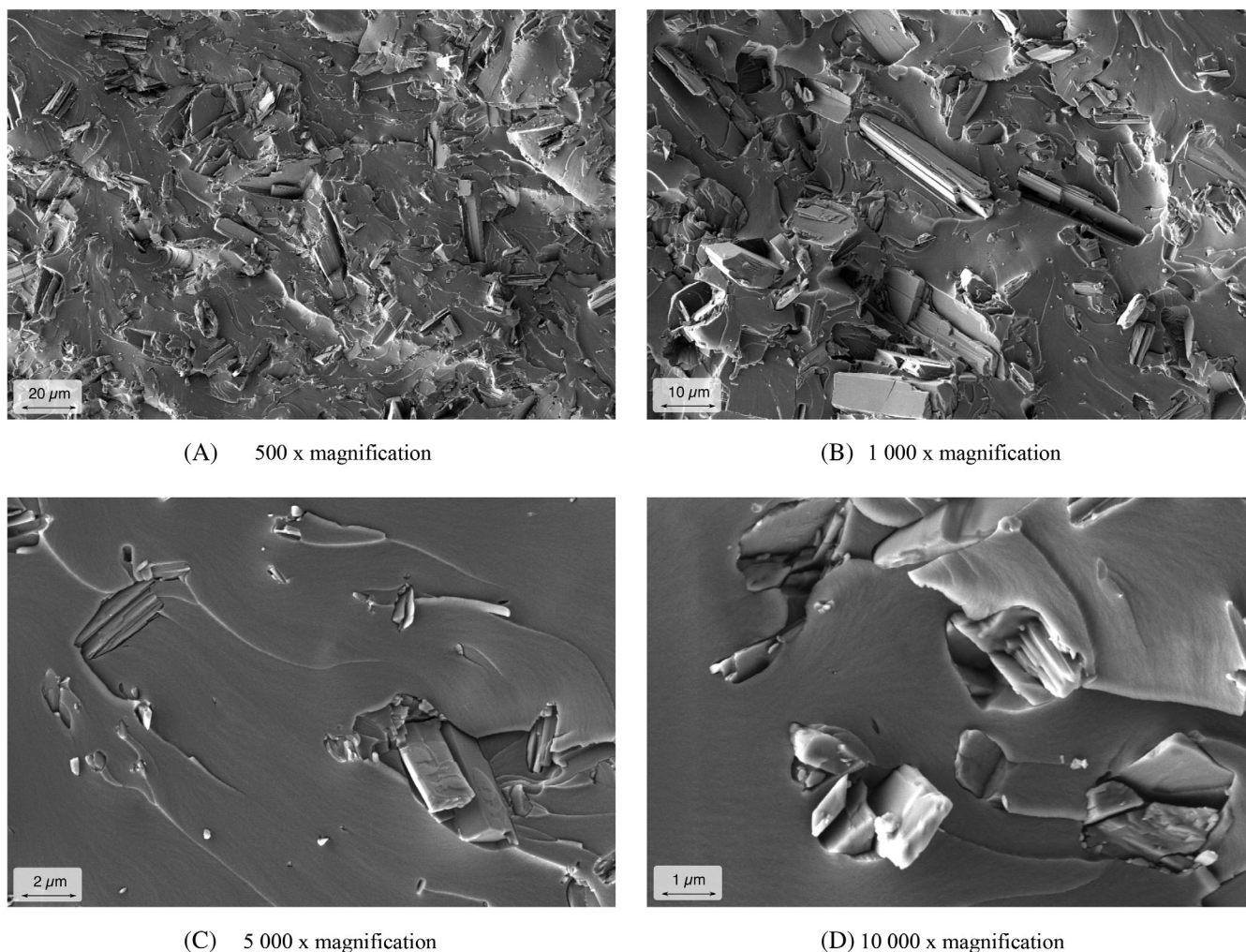
(A) 500 x magnification

(B) 1 000 x magnification

(C) 5 000 x magnification

(D) 10 000 x magnification

FIGURE 4 Fracture surface of compact tension specimen made from T10 at 500 x (A), 1000 x (B), 5000 x (C), and 10,000 x magnification (D).

Figure 4B provides a more detailed view of the amino acid crystals. Interestingly, the crystals exhibit an oblong shape resembling short rods. Agglomerates of filler particles typically do not exhibit preferential direction and tend to be more spherical.[33–35] This strengthens the assumption that the particles possess a crystalline nature and may have formed during the curing of the thermoset. Furthermore, the crystals display a layered structure with individual layers oriented along the longitudinal axes of the crystals. The surface of the individual layers appears smooth, and the fracture surface is predominantly oriented along the longitudinal axes of the crystals.

Figure 4C offers a close-up view of the thermoset's fracture surface. Here, characteristic patterns and crystals with sizes well below 1 μm can be observed. The presence of lines and voids formed during crack propagation suggests the activation of toughening mechanisms such as crack bridging, particle pull-out, crack pinning, crack deflection, and crack bifurcation.[36,37] Rothenhäusler et al. already proposed the presence of different toughening mechanisms in DGEBA cured with L-arginine at different testing temperatures.[18] However, the definitive investigation of these toughening mechanisms and their contribution to the thermoset's toughness are beyond the scope of this study.

Figure 4D displays crystals ranging in size from 100 nm to 1 μm. It is evident that the adhesion between the crystals and the surrounding thermoset matrix varies, ranging from poor to non-existent, with visible gaps between the thermoset and crystals. This could be a result of differences in thermal expansion or contraction during cooling of the thermoset after curing, or it may be due to more pronounced shrinkage during the formation of crystals compared to the matrix. The analysis of crystal size, morphology, and adhesion provides valuable insights into the microstructure of the epoxy resin cured
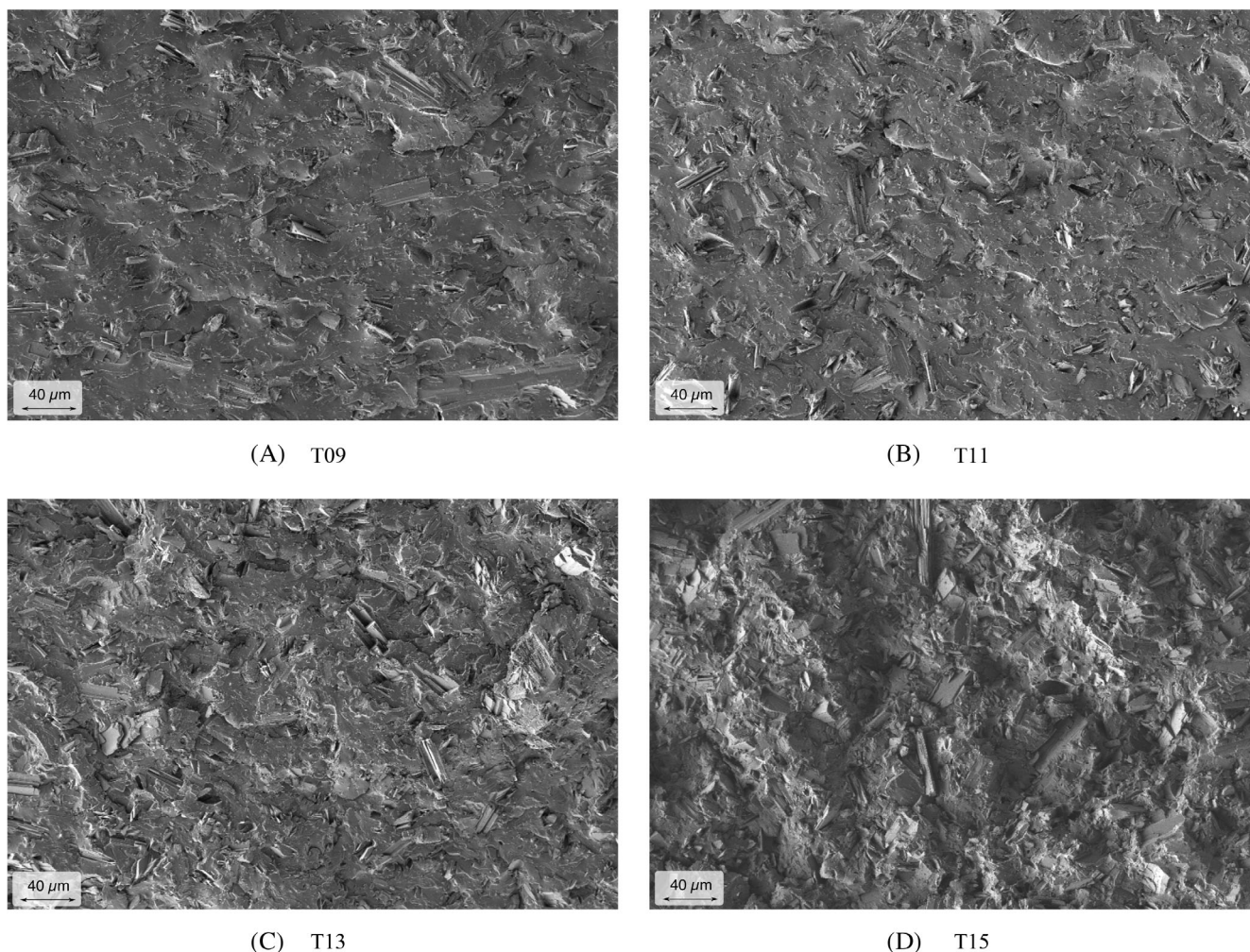
FIGURE 5   Fracture surface of compact tension specimen made from T09 (A), T11 (B), T13 (C), and T15 (D) at 250 x magnification.

with L-tyrosine. These observations contribute to understanding the mechanisms behind the improved mechanical properties observed in the thermosets and provide a foundation for further investigation into toughening mechanisms and their influence on the overall performance of the material.

Figure 5 presents SEM images of the fracture surfaces of compact tension specimens made from DGEBA cured with L-tyrosine at different R values at 250 x magnification. The images clearly demonstrate that an increased weight fraction of L-tyrosine results in a greater number of crystals on the fracture surface. It is worth noting that as the R value increases, there may be a decrease in the number of crystals with sizes around 1 μm. However, due to the significant coverage of the fracture surface by amino acid crystals in the T15 specimen, it becomes challenging to precisely assess this aspect. Consequently, the addition of more L-tyrosine to the epoxy matrix primarily increases the number of crystals present, while the network structure, or cross-link density, of the surrounding matrix remains unchanged, as demonstrated in Section 3.3. This

conclusion aligns with the findings of Section 3.1, which indicate that the amount of L-tyrosine incorporated into the thermoset network during curing ($C_{\text{tyrosine,cure}}$) remains relatively constant across a wide range of R values.

As the R value increases, the perceived surface roughness also intensifies, leading to an augmented fracture toughness. This can be attributed to the longer distance the crack needs to propagate due to the increased surface roughness. The surface texture undergoes a transformation from a fine-grained appearance with individual amino acid particles exposed by the crack to a coarser fracture surface. Overall, these observations highlight the influence of L-tyrosine content on the fracture surfaces and surface roughness of the cured thermosets, ultimately affecting their fracture toughness.

3.3 | Dynamic Mechanical Analysis

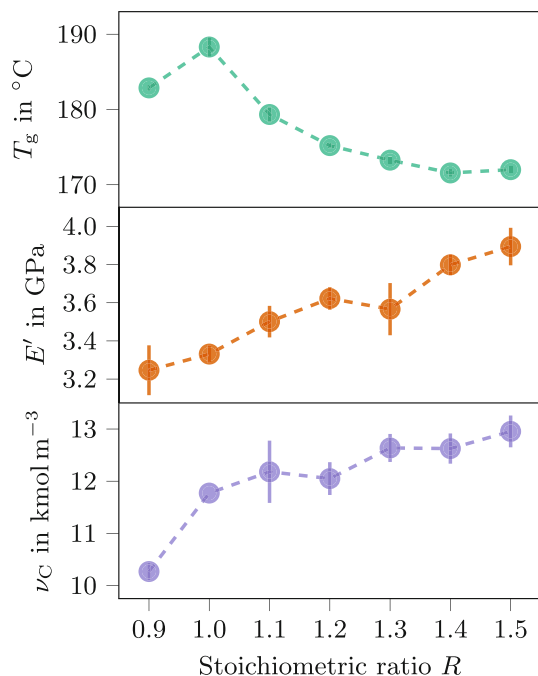After investigating the X_c as well as the crystal morphology and the crystal size distribution in the

FIGURE 6 Glass transition temperature T_g, storage modulus E' at T = 22°C, and cross-link density ν_C of DGEBA cured with different R of L-tyrosine.

FIGURE 7 Flexural modulus E_F, flexural strength σ_F, and fracture strain ε_F of DGEBA cured with different R of L-tyrosine.

different thermosets, the influence of the varying R and X_c on the T_g, E' at T = 22°C and the ν_C of DGEBA cured with L-tyrosine is analyzed (see Figure 6). The T_g of the thermosets shows a slight increase from 182.8°C (T09) to 188.3°C (T10) as the R value increases. However, for further increases in R, the T_g decreases continuously to 171°C (T15). This indicates that R has an influence on the T_g of epoxy resins cured with L-tyrosine. Nevertheless, the effect of R on T_g is relatively small compared to the changes observed in epoxy resins cured with conventional, petroleum-based amine curing agents.[8,9] This suggests that the addition of more L-tyrosine does not lead to significant changes in the network structure. Instead, L-tyrosine tends to separate from the resin and form crystals, as discussed in Sections 3.1 and 3.2. Therefore, the network structure itself is less dependent on R, and excess L-tyrosine will preferentially form crystals rather than affecting the network structure.

It is worth noting that all compositions exhibit a T_g higher than 170°C. This high T_g is likely due to steric hindrance caused by the phenyl group of L-tyrosine, as discussed in a previous study.[19] Interestingly, T10, which was previously discussed for its mechanical properties, exhibits the highest T_g. However, since L-tyrosine separates from the epoxy resin, this observation does not necessarily provide information about the correct number of active hydrogen atoms in L-tyrosine.
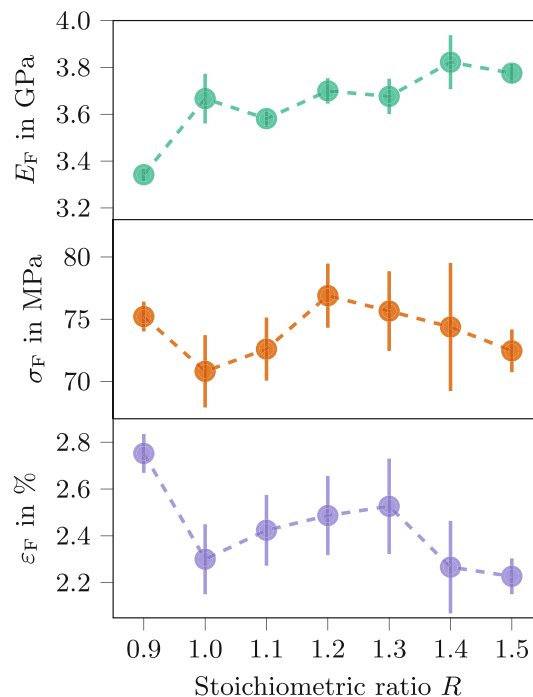
As a result of the higher X_c with higher R (see Section 3.1 and 3.2), the E' of the thermosets increase almost linearly from 3.2 GPa for T09 to 3.9 GPa for T15. In general, amino acid crystals have a significantly higher modulus than thermosets and, therefore, act as a reinforcement in the polymeric matrix.[38–40] Using atomic force microscopy nano-indentation, Ji et al. determined the Young's modulus of L-tyrosine crystals to be 177 GPa.[25] In contrast, Adhikari et al. found a Young's modulus of 42 GPa.[41] Thus, the L-tyrosine crystals act as bio-based, particulate reinforcement in the thermoset matrix.

However, this also influences E' in the rubbery state of the thermoset which could explain the drastic increase in ν_C with higher R. Therefore, no reliable information can be obtained from analyzing the absolute magnitude ν_C of a filled, that is, reinforced, thermoset. Still, relative changes in ν_C of epoxy resins cured with amino acids as the result of different curing regimes for the same composition may deliver important information about the network structure.

3.4 | Three-point bending

Figure 7 shows the flexural modulus (E_F), flexural strength (σ_F), and fracture strain (ε_F) of DGEBA cured with different R of L-tyrosine. Similar to the trend of E',
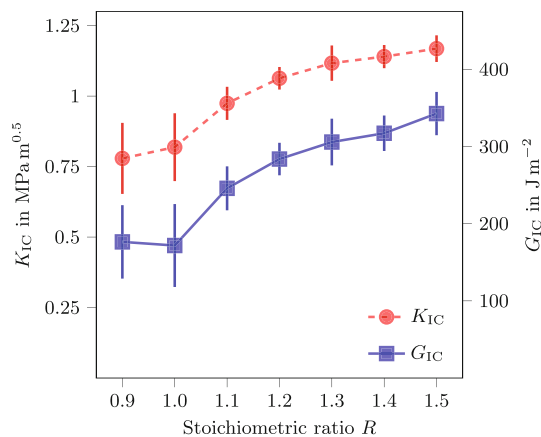
FIGURE 8 Critical stress intensity factor in mode I K_{IC} and fracture energy G_{IC} of DGEBA cured with different R of L-tyrosine.

FIGURE 9 Pearson product–moment correlation coefficients R_P of the stoichiometric ratio R, degree of crystallinity X_c, glass transition temperature T_g, storage modulus E', cross-link density ν_C, critical stress intensity factor in mode I $K_{IC,}$ and fracture energy G_{IC} of DGEBA cured with different R values of L-tyrosine.

E_F increases from about 3.3 GPa for T09 to 3.8 GPa for T15. However, the relationship between E_F and R is not as linear as the changes observed in E'. Notably, there is a significant increase in E_F from T09 to T10. As already discussed in section 3.3, E_F is significantly increased by the reinforcement of the L-tyrosine crystals. However, the increase in E_F with higher X_c (as described in Section 3.1) is relatively low due to the low aspect ratio and random, three-dimensional orientation of the crystals, which limits their reinforcing effect.[42–44] Nevertheless, the E_F values are significantly higher than those of epoxy resins cured with conventional amine curing agents, which typically have E_F values not exceeding 2.8 GPa.

The σ_F of all thermosets ranges between 71 MPa to 77 MPa. Compared to DGEBA cured with petroleum-based amine curing agents, the σ_F of the tested thermosets are comparatively low.[45] The images in Section 3.2 show that the adhesion between amino acid crystals and the surrounding matrix is poor. Therefore, the L-tyrosine crystals might act as defects in the matrix, leading to stress concentrations in their vicinity. The strain at failure is comparatively low for an epoxy resin-based thermoset and likely linked to the stress concentrations caused by the L-tyrosine crystals.

Similar to the results of Section 3.3, the changes in the flexural properties as the result of the different R are small compared to ones observed in other investigations and can be mainly attributed to the changes in X_c.[9–12]

3.5 | Fracture toughness

As discussed in Sections 3.1 and 3.2, the X_c and fracture surface roughness of the thermosets increase with higher R values. Consequently, the weight fraction of toughening agent, particularly L-tyrosine crystals, increases,
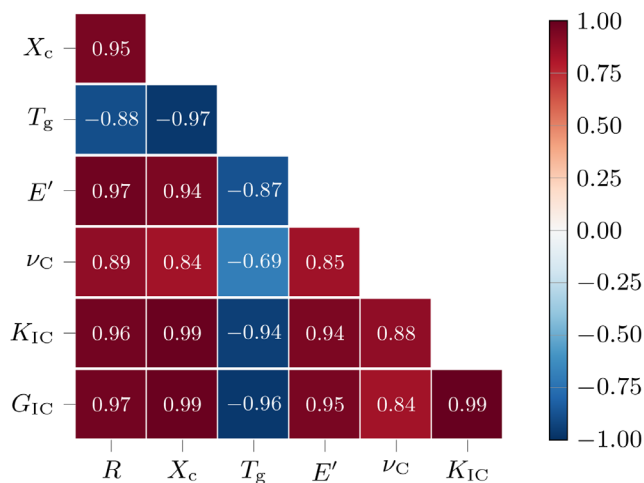
leading to an enhancement in the fracture toughness properties of the thermosets. The fracture toughness, represented by K_{IC} and G_{IC}, shows a continuous increase with increasing R. K_{IC} increases steadily from 0.78 MPam$^{0.5}$ for T09 to 1.17 MPam$^{0.5}$ for T15 (see Figure 8). Similarly, G_{IC} increases 177 J/m^2 for T09 to 343 J/m^2 for T15. This indicates that adding more amino acid particles to the thermoset progressively enhances its resistance to unstable crack propagation and increases the energy dissipated during crack growth. Further details regarding the toughening mechanism and fracture surface morphology can be found in Section 3.2.

It is noteworthy that the K_{IC} and G_{IC} of T10 are already significantly higher than that of a liquid epoxy resin cured with dicyandiamide, which typically range from 0.6 to 0.7 MPam$^{0.5}$.[46–48] In epoxy resin systems toughened with layered silica, liquid rubbers and core-shell particles,[49–52] there is an optimal filler content for high toughness. In conclusion, for the system studied in this investigation, the optimal filler content for high toughness is at or above the stoichiometric ratio of $R = 1.5$.

3.6 | Structure–property relationships

Lastly, structure–property relationships are derived by correlating the results of DSC, DMA, and compact tension tests. The Pearson product–moment correlation coefficients (R_P)[53] (see Figure 9) of the stoichiometric ratio R, degree of crystallinity X_c, glass transition temperature T_g, storage modulus E', cross-link density ν_C, critical stress

intensity factor in mode I K_{IC} and fracture energy G_{IC} of DGEBA cured with different R of L-tyrosine are calculated via *numpy.corrcoef()* in *Python 3.8.0*.[54]

Firstly, it is important to discuss the correlations between R and the crucial structural properties X_c and ν_C. Here, R correlates strongly with X_c ($R_P = 0.95$) because higher amounts of L-tyrosine in the formulation lead to a more pronounced formation of amino acid crystals. This might be a result of the limited solubility of L-tyrosine in DGEBA. Thermodynamically, crystals are more stable than their amorphous counterparts and the resin system can lower its internal energy by separating the amino acid from the epoxy resin matrix.[55]

Here, larger crystals are formed most likely from nano-meter-sized L-tyrosine particles via Ostwald ripening.[56] Thereby, the total free surface between DGEBA and L-tyrosine particles is decreased and the surface energy is lowered.[57]

On the other hand, ν_C also correlates positively with R ($R_P = 0.89$). However, this is mainly caused by the reinforcing effect of the L-tyrosine crystals in the thermoset matrix. As already described, L-tyrosine crystals have a higher Young's modulus than the surrounding matrix.[25,41] Therefore, the crystals act as particle reinforcement and increase the thermosets' modulus in the rubbery state. There is a strong anti-correlation ($R_P = -0.88$) between T_g and R because some of the excess L-tyrosine stays in the epoxy matrix and thereby modifies the network structure, which leads to a decrease of T_g.

Next, X_c has a positive correlation with E' ($R_P = 0.94$) because the L-tyrosine crystals have a high Young's modulus and act as reinforcements in the matrix. Remarkably, X_c correlates almost perfectly with K_{IC} ($R_P = 0.99$) and G_{IC} ($R_P = 0.99$), showing that the toughness increase at higher R is mostly dependent on the higher fraction of crystals in the thermoset matrix.

4 | CONCLUSION

The present study aimed to investigate the impact of the stoichiometric ratio on crystal formation, network structure, and resulting mechanical properties of DGEBA cured with L-tyrosine. The existence of amino acid crystals in the thermoset matrix and their effects on the thermoset's mechanical performance are elucidated for the first time in the literature. Upon increasing R, a greater abundance of L-tyrosine crystals was observed, serving as reinforcements within the epoxy matrix. As a result, the network structure and glass transition temperature displayed only marginal changes compared to epoxy resins cured with conventional amine curing agents. Notably, the flexural strength and strain at failure exhibited insignificant variations. Interestingly, the addition of additional L-tyrosine to the resin resulted in an augmented fracture toughness, indicating the toughening capabilities of L-tyrosine crystals. As a result, the amino acid act not only as a curing agent but also as a toughening agent. Consequently, further incorporation of L-tyrosine into the thermoset material proved advantageous, enhancing its overall mechanical performance. Here, the composition with a stoichiometric ratio of $R = 1.5$ has the highest fracture toughness of the formulations that were tested.

DATA AVAILABILITY STATEMENT
The data that support the findings of this study are available from the corresponding author upon reasonable request.

ORCID
Florian Rothenhäusler https://orcid.org/0000-0001-9948-3310
Holger Ruckdaeschel https://orcid.org/0000-0001-5985-2628

REFERENCES
1. Flemming M, Ziegmann G, Roth S. *Faserverbundbauweisen—Fasern und Matrices*. Springer; 1995.
2. Lengsfeld H, Altstädt V, Wolff-Fabris F, Krämer J. *Composite Technologien*. Carl Hanser Verlag GmbH & Co. KG; 2014.
3. Ashcroft W. *Epoxy Resins—Chemistry and Technology*. Chapter 2, 37–71. Springer; 1993.
4. Pham H, Marks M. Epoxy Resins. *Ullmann's Encycl Ind Chem*. 2004;13:156.

5. Lau CH, Hodd KA, Wright WW. Structure and properties relationships of epoxy resins part 1: crosslink density of cured resin: (II) model networks properties. *Br Polym J*. 1986;18(5):316-322.

6. Levita G, De Petris S, Marchetti A, Lazzeri A. Crosslink density and fracture toughness of epoxy resins. *J Mater Sci*. 1991;26:2348-2352.

7. Espuche E, Galy J, Gérard J-F, Pascault J-P, Sautereau H. Influence of crosslink density and chain flexibility on mechanical properties of model epoxy networks. *Macromol Symp*. 1995;93(1):107-115.

8. Murayama T, Bell J. Journal of polymer science part A-2: polymer. *Phys Ther*. 1970;8(3):437-445.

9. Gupta VB, Drzal LT, Lee CY-C, Rich MJ. The temperature-dependence of some mechanical properties of a cured epoxy resin system. *Polym Eng Sci*. 1985;25(13):812-823.

10. Palmese GR, McCullough RL. Effect of epoxy–amine stoichiometry on cured resin material properties. *J Appl Polym Sci*. 1992;46(10):1863.

11. Meyer F, Sanz G, Eceiza A, Mondragon I, Mijovic J. The effect of stoichiometry and thermal history during cure on structure and properties of epoxy networks. *Polymer*. 1995;36(7):1407-1414.

12. Fernandez-Nograro F, Valea A, Llano-Ponte R, Mondragon I. Dynamic and mechanical properties of DGEBA/poly(propylene oxide) amine based epoxy resins as a function of stoichiometry. *Eur Polym J*. 1996;32(2):257-266.

13. Leuchtenberger W, Huthmacher K, Drauz K. Biotechnological production of amino acids and derivatives: current status and prospects. *Appl Microbiol Biotechnol*. 2005;69:1-8.

14. Nelson D, Cox M. *Lehninger Principles of Biochemistry*. MacMillan Learning; 2021.

15. Li Y, Xiao F, Moon K, Wong C. Novel curing agent for lead-free electronics: Amino acid. *J Polym Sci, Part A: Polym Chem*. 2005;44:1020-1027.

16. Shibata M, Fujigasaki J, Enjoji M, Shibita A, Teramoto N, Ifuku S. Amino acid-cured bio-based epoxy resins and their biocomposites with chitin- and chitosan-nanofibers. *Eur Polym J*. 2018;98:216-225.

17. Rothenhäusler F, Ruckdaeschel H. L-arginine as a bio-based curing agent for epoxy resins: glass transition temperature, rheology and latency. *Polymers*. 2022;14:20.

18. Rothenhäusler F, Ruckdaeschel H. L-arginine as bio-based curing agent for epoxy resins: temperature-dependence of mechanical properties. *Polymers*. 2022;14:21.

19. Rothenhäusler F, Ruckdaeschel H. Amino acids as bio-based curing agents for epoxy resin: correlation of network structure and mechanical properties. *Polymers*. 2023;15:2.

20. Albuquerque RQ, Rothenhäusler F, Ruckdaeschel H. Designing formulations of bio-based, multi-component epoxy resin systems via machine learning. *MRS Bull*. 2023;1:1.

21. Mazzocchetti L, Merighi S, Benelli T, Giorgini L. AIP Conference Proceedings. 020170. 2018.

22. Merighi S, Mazzocchetti L, Benelli T, Giorgini L. Evaluation of novel bio-based amino curing agent Systems for Epoxy Resins: effect of tryptophan and guanine. *Processes*. 2021;9:42.

23. Li Y, Xiao F, Wong C. Novel, environmentally friendly crosslinking system of an epoxy using an amino acid: Tryptophan-cured diglycidyl ether of bisphenol A epoxy. *J Polym Sci Part A: Polym Chem*. 2007;45:181-190.

24. Motahari A, Rostami A, Omrani A, Ehsani M. On the thermal degradation of a novel epoxy-based nanocomposite cured with tryptophan as an environment-friendly curing agent. *J Macromol Sci Phys*. 2015;54:5-532.

25. Ji W, Xue B, Arnon ZA, et al. Rigid tightly packed amino acid crystals as functional supramolecular materials. *ACS Nano*. 2019;13(12):14477-14485.

26. Cease H, Derwent P, Diehl H, Fast J, Finley D. Measurement of Mechanical Properties of Three Epoxy Adhesives at Cryogenic Temperatures for CCD Construction. 2006.

27. Weiss IM, Muth C, Drumm R, Kirchner HOK. Thermal decomposition of the amino acids glycine, cysteine, aspartic acid, asparagine, glutamic acid, glutamine, arginine and histidine. *BMC Biophys*. 2018;11(1):2.

28. Bird RB, Stewart WE, Lightfoot EN. *Transport Phenomena*. Wiley; 2007.

29. Chernov AA. *Crystal Growth*. North-Holland; 2004.

30. Einstein A. Ph.D. thesis, University of Zurich. 1905.

31. Doi M, Edwards SF. *Suspensions of Colloidal Particles and Aggregates*. Cambridge University Press; 1996.

32. Farkas A, Strohm PF. Imidazole catalysis in the curing of epoxy resins. *J Appl Polym Sci*. 1968;12(1):159-168.

33. Inam F, Peijs T. Re-aggregation of carbon nanotubes in two-component epoxy system. *J Nanostruct Polym Nanocompos*. 2006;2:86.

34. Jux M, Finke B, Mahrholz T, Sinapius M, Kwade A, Schilde C. Effects of Al(OH)O nanoparticle agglomerate size in epoxy resin on tension, bending, and fracture properties. *J Nanopart Res*. 2017;19(4):139.

35. Kurimoto M, Yoshida S, Umemoto T, Mabuchi T, Muto H. 2019 IEEE Conference on Electrical Insulation and Dielectric Phenomena (CEIDP), 360–363. 2019.

36. Wetzel B, Rosso P, Haupert F, Friedrich K. Fracture of polymers, composites and adhesives. *Eng Fract Mech*. 2006;16:2375.

37. Zotti A, Zuppolini S, Zarrelli M, Borriello A. *Fracture Toughening Mechanisms in Epoxy Adhesives*, ISBN 978-953-51-2783-3. In: Anna R, ed. Adhesives - Applications and Properties. IntechOpen; 2016. doi:10.5772/65250

38. Azuri I, Meirzadeh E, Ehre D, et al. Unusually large young's moduli of amino acid molecular crystals. *Angewandte Chemie (International ed. in English)*. 2015;54(46):13566-13570.

39. Basavalingappa V, Bera S, Xue B, et al. Diphenylalanine-derivative peptide assemblies with increased aromaticity exhibit metal-like rigidity and high piezoelectricity. *ACS Nano*. 2020;14(6):7025-7037.

40. Karothu DP, Dushaq G, Ahmed E, et al. Mechanically robust amino acid crystals as fiber-optic transducers and wide band-pass filters for optical communication in the near-infrared. *Nat Commun*. 2021;12(1):1326.

41. Adhikari RY, Pujols JJ. Highly rigid & transparent supramolecular fibrils of tyrosine. *Nano Select*. 2022;3(9):1314-1320.

42. Halpin JC, Kardos JL. The Halpin-Tsai equations: a review. *Polym Eng Sci*. 1976;16(5):344-352.

43. Pan N. The elastic constants of randomly oriented fiber composites: a new approach to prediction. *Sci Eng Compos Mater*. 1996;5(2):63.

44. Mcnally D. Short fiber orientation and its effects on the properties of thermoplastic composite materials. *Polym-Plast Technol Eng*. 2008;8:101-154.

45. Garcia FG, Soares BG, Pita VJRR, Sánchez R, Rieumont J. Mechanical properties of epoxy networks based on DGEBA and aliphatic amines. *J Appl Polym Sci*. 2007;106(3):2047-2055.

46. Varley RJ. Toughening of epoxy resin systems using low-viscosity additives. *Polym Int*. 2004;53(1):78-84.

47. Kim BC, Park SW, Lee DG. Fourteenth international conference on composite structures. *Compos Struct*. 2008;86:1-69.

48. Hübner F, Hoffmann M, Sommer N, et al. Temperature-dependent fracture behavior of towpreg epoxy resins for cryogenic liquid hydrogen composite vessels: the influence of polysiloxane tougheners on the resin yield behavior. *Polym Test*. 2022;113:107678.

49. Han J, Cho K. Layered silicate-induced enhancement of fracture toughness of epoxy molding compounds over a wide temperature range. *Macromol Mater Eng*. 2005;290:1184-1191.

50. Quan D, Ivankovic A. Effect of core–shell rubber (CSR) nanoparticles on mechanical properties and fracture toughness of an epoxy polymer. *Polymer*. 2015;66:28.

51. Utz J, Kunz R, Breu J, Altstädt V. Influence of particle size on toughening mechanisms of layered silicates in CFRP. *Materials*. 2020;13:2396.

52. Neves RM, Ornaghi HL, Zattera AJ, Amico SC. Toughening epoxy resin with liquid rubber and its hybrid composites: a systematic review. *J Polym Res*. 2022;29(8):340.

53. Bravais A. *Analyse mathématique sur les probabilités des erreurs de situation d'un point*. Impr. Royale; 1844.

54. NumPy-Developers, numpy.corrcoef()-function, Website, Taken. 2023 https://numpy.org/doc/stable/reference/generated/numpy.corrcoef.html

55. Chaikin PM, Lubensky TC. *Principles of Condensed Matter Physics*. Cambridge University Press; 1995.

56. Thanh NTK, Maclean N, Mahiddine S. Mechanisms of nucleation and growth of nanoparticles in solution. *Chem Rev*. 2014;114(15):7610-7630.

57. Ostwald W. Über die vermeintliche Isomerie des roten und gelben Quecksilberoxyds und die Oberflächenspannung fester Körper. *Z fur Phys Chem*. 1900;34U(1):495-503.